Effect of annealing temperature on microstructure, mechanical and tribological properties of nano-SiC reinforced Ni-P coatings

Qianzhi Wang[a*], Mauro Callisti[a], Jake Greer[a], Brian McKay[b], Tatjana Kosanovic Milickovic[c], Alexandros Zoikis-Karathanasis[c], Ioanna Deligkiozi[d], Tomas Polcar[a]

[a] National Centre for Advanced Tribology at Southampton, Department of Mechanical Engineering, Faculty of Engineering and the Environment, University of Southampton, Southampton SO17 1BJ, UK

[b] Institute of Materials and Manufacturing, Brunel University, London UB8 3PH, UK

[c] Centre for Research and Technology Hellas (CERTH/IRETETH), Trikala GR42100, Greece

[d] Centre for Technology Research and Innovation, Limassol 3106, Cyprus

Abstract: The tribological properties of Ni-P/SiC nanocomposite coatings annealed at different temperatures (350-500 ℃) were investigated in order to determine the optimal temperature needed to enhance their wear resistance as well as to reveal the underlying wear mechanisms. With increasing annealing temperature, the hardness of the annealed coatings gradually decreased from 8.2±0.5 to 7.1±0.6 GPa as a result of the Hall-Petch effect, nevertheless these values obtained were constantly higher than that of the as-plated coating (6.3±0.3 GPa) due to the formation of a hard Ni_3P phase. Regarding to tribological properties, the Ni-P/SiC coating annealed at 350 ℃ presented a poorer wear resistance (6.1×10^{-5} mm^3/Nm) compared to the as-plated coating (3.9×10^{-5} mm^3/Nm) owing to a rougher original contact surface and the subsequent generation of nickel and iron oxides on the wear track. In contrast, coatings annealed at temperatures ranging between 400-500 ℃ exhibited the improved wear resistance (4.3×10^{-5}-7.8×10^{-6} mm^3/Nm) attributable to their smoother surfaces and to the lubrication effect of H_3PO_4 arising from the tribochemical reaction between Ni_3P and the environment. Overall, the Ni-P/SiC coating annealed at 500 ℃ containing the largest amount of Ni_3P exhibited the lowest friction coefficient (0.51) and wear rate (7.8×10^{-6} mm^3/Nm).

***Keywords*:** Nickel-phosphorus; SiC; Electroplating; Tribology; Annealing.

1. Introduction

Protective coatings have attracted scientific interest for decades due to their potential to increase resistance to wear and corrosion, which are estimated to account for 3-4% of the world's Gross Domestic Product (GDP) [1]. At present, one of the mostly used coatings in the world is hard chrome,

* Corresponding author. Tel.: +44-23-8059-4438.
E-mail address: qz.wang@soton.ac.uk; jxwqz1985@aliyun.com.

as it exhibits a unique property that simultaneously helps prevent wear and corrosion. However, Cr^{6+} (hexavalent chromium) used in electrolytic baths is extremely harmful to both human health and the environment [2]. As a result, hard chrome electroplating must be accompanied by expensive ventilation and complicated waste management systems in order to meet strict legislations [3]. Consequently, Ni-P coatings employing the same deposition technique were introduced, and the influence of the baths parameter [4], surfactant [5], pH value [6] and post-treatments such as hydrogen plasma [7] and annealing [8] on their comprehensive properties were investigated. Optimised Ni-P coatings are well suited for general applications, especially in corrosive environments, but their hardness and wear resistance are still inadequate for more demanding situations. Hence, various reinforcing particles such as SiC [9, 10], TiN [11], TiO_2 [12], SiO_2 [13], WC [14], Al_2O_3 [15], B_4C [16] and CNTs [17] were incorporated into Ni-P coatings to enhance their mechanical and tribological properties. As reported in Table 1, incorporation of reinforcing particles increases the hardness of Ni-P coatings, especially when SiC particles were used. Moreover, studies [18, 19] have demonstrated that the incorporation of SiC particles in a Ni-P matrix is the most effective combination of cost and performance in industrial applications.

Regarding Ni-P/SiC composite coatings, SiC particles with a size ranging between 0.5-6.0 μm was mostly used [20-25], while only a few studies investigated the use of nano-sized SiC particles (40-50 nm) [26-32]. However, it is worth noting that these studies investigated only the effects of SiC nanoparticles on the microstructures, corrosion resistance [26-30] and wear resistance of the as-plated coatings [31, 32]. Therefore, there is still a large gap in the relationship between microstructure, mechanical and tribological properties of Ni-P/(nano)SiC coatings. In particular, the effects of post-deposition heat treatments on the tribological properties is still unexplored.

In this study, SiC particles with a nanometric size were incorporated in Ni-P coatings, and the effects of different annealing temperatures on the microstructure, mechanical and tribological properties of the composite coatings was investigated and correlated.

2. Experiment details

2.1 Coatings electroplating

Plasma CVD β-SiC particles (density of 3.22 g/cm^3, Nanostructured & Amorphous Materials, Inc.) with a size ranging between 45-55 nm were used as reinforcement for Ni-P coatings. Carbon steel plate substrates, with a size of 4×6 cm^2 and a thickness of 1 mm were cleaned in solvent, alkaline and acid washes. Before depositions, the substrates were covered with galvanic tape (3M 470 Electroplating and Anodizing Vinyl Tape) so as to leave a 4×4 cm^2 exposure area. Direct current (DC) electroplating was performed under a constant current density of 20 A·dm^{-2}, with the carbon steel plates acting as cathodes and the Ni-S balls in titanium mesh baskets as anodes. In order to ensure a uniform electrolyte solution, a magnetic stirring at 300 rpm was applied. Ni-P/SiC composite coatings (5.9 wt% P) ~ 60 μm thick were electroplated from a bath containing nickel sulphate as the nickel source, phosphorous acid as P source, nickel chloride to support the dissolution of Ni-S anode, as well as wetting, buffering and dispersing agents. The deposition parameters for the fabrication of Ni-P/SiC composite coatings are listed in Table 2.

The as-plated Ni-P/SiC coatings (50 ℃) were subsequently annealed at 350, 400, 450 and 500 ℃. Hereafter, samples annealed at different temperatures are denoted as Ni-P/SiC-50, Ni-P/SiC-350, Ni-P/SiC-400, Ni-P/SiC-450 and Ni-P/SiC-500, respectively. During the heat treatment, a constant heating rate of 5 ℃/min was maintained until the designated temperature was reached, and all samples were isothermally annealed at the target temperature for 1 hour before cooling naturally to room temperature. As the isothermal annealing was conducted in an electric furnace followed by air-cooling, a thin oxide layer formed on the top surface of the coatings. In order to remove the residual surface oxides, after the heat treatments the samples were polished by using a 0.3 μm Al_2O_3 colloidal solution for 5 minutes.

2.2 Characterization of microstructure and mechanical properties

The surface morphology of Ni-P/SiC coatings after polishing was examined by using a FEG-SEM (JEOL-JSM-6500F, Japan) while the chemical composition of the deposits was measured by using energy dispersive X-ray spectroscopy (FEI Quanta 200, Netherland). Moreover, SiC

nanoparticles were observed by SEM (Zeiss). Microstructural analyses were carried out by X-ray diffraction (XRD) with a Cu-K_α radiation (Siemens D-5000). XRD data were recorded for 2θ ranging between 20 °-100 ° with a scan step size of 0.05 ° at a scan rate of 5 °/min. A nanoindenter (Micromaterials, Wrexham, UK) equipped with a diamond Berkovich tip was used to measure the mechanical properties of Ni-P/SiC coatings. In order to minimize substrate effects a penetration depth of 500 nm (less than 1% of coatings thickness) was used. At least 10 indents were performed on each coating for statistical analyses. Hardness (*H*) and reduced elastic modulus (E_r) were calculated from the load-displacement curves according to the procedure outlined by Oliver and Pharr

2.3 Tribological properties

A reciprocating tribometer (TE77, Phoenix Tribology, Ltd.) was used to evaluate the tribological properties of Ni-P/SiC coatings. Based on the potential application of Ni-P/SiC coatings on crankshaft and piston ring, 52100 steel balls (Ø 6 mm) as a material for making linkage (against crankshaft) and cylinder (against piston ring) were used as counterparts in this study. In order to obtain a steady friction coefficient after the running-in stage and before coatings failure, the load and frequency were kept at 10 N and 5 Hz, respectively over a stroke of 10 mm and for a sliding time of 1 hour. Accordingly, a line velocity of 0.1 m/s and a total sliding distance of 360 m were covered. To ensure the validity of collected frictional data, two tribotests were carried out for each coating, while a third test was carried out when the relative error was over 5 %.

After tribotests, the wear scars on counterparts and coatings were measured by a 3D optical microscope (Infinite Focus, Alicona, UK). The wear volume of the balls was assessed using Eq. (1), while the wear volume of the coatings was calculated by taking into account the cross-section (*A*) and the length (*L*) of wear track.

$$V = \frac{\pi d^4}{64\mathrm{R}} \quad (1)$$

In Eq. (1), d and R are the diameter of wear scar and the radius of the steel ball, respectively. Moreover, the morphology of wear track was observed by FEG-SEM (JEOL-JSM-6500F, Japan), and its composition was analyzed using EDS (Inca Energy 350, Oxford, UK).

3. Results and discussions

3.1 Microstructure

SiC particles exhibited a spherical shape (Fig.1a) and a cubic crystalline structure (Fig.1b), which demonstrates their high purity (97.5 %). As seen in Fig.2a, all of the Ni-P/SiC coatings exhibited two main diffraction peaks attributed to Ni (111) and Ni (222) around 44.43 ° and 98.33 °, respectively (reference: JCPDS 04-0850). The intensity of these peaks increased significantly after annealing, thus suggesting a higher degree of crystallinity for Ni in Ni-P/SiC coatings. Accordingly, the crystallite size calculated from the Ni (111) peak by using the Scherrer's formula also increased in relation to the annealing temperature (Fig.2b). On the other hand, after annealing a weak peak (2θ~60.16 °) attributed to a Ni_3P phase appeared in the XRD pattern for the Ni-P/SiC-350 coating, while the XRD pattern was more densely populated by peaks attributed to Ni_3P when the annealing temperature exceeded 350 ℃ (Fig.2a). Structural properties of Ni-P/SiC-50 and Ni-P/SiC-450 coatings were extracted from the XRD patterns by using a Difrac® plus Eva software and listed in Table 3. In spite of a high number of Ni_3P peaks observed in the diffractograms, the fraction of Ni_3P was still limited due to the low concentration of phosphorus in Ni-P/SiC coatings (5.9 wt%). The surface morphology of polished Ni-P/SiC coatings (Fig.3) became smoother with increasing annealing temperature, thus affecting the frictional behavior of the coatings, as will be discussed in the following sections.

3.2 Characterization of mechanical property

Hardness (H) and reduced elastic modulus (E_r) of Ni-P/SiC coatings were calculated from the load-displacement curves after that these were corrected by taking into account thermal drift and frame compliance. Table 4 summarizes calculated mechanical properties. Annealed coatings exhibited a higher average hardness (7.1 ±0.6-8.2 ±0.5 GPa) compared to the Ni-P/SiC-50 coating (6.3 ±0.3 GPa). The hardness increase is attributed to the formation of a hard Ni_3P phase [33]. Nevertheless, the hardness of Ni-P/SiC coatings decreased gradually from 8.2 GPa to 7.1 GPa as the annealing temperature was increased from 400 to 500 ℃. The observed decrease in hardness is

attributed to the increasing grain size of the Ni (111) phase according to the Hall-Petch effect [34]. Wear resistance is often correlated to mechanical parameters such as H/E_r and H^3/E_r^2 ratios, which provide simultaneous information about resistance to plastic deformation and elastic properties of materials [35]. Based on these parameters (Tab. 4), the coating annealed at 400 ℃ is expected to exhibit the best tribological performance.

3.3 Frictional properties

Fig. 4a shows some representative friction curves measured on coatings annealed at different temperatures. It is seen that the friction coefficient of coatings annealed at temperatures ≤ 450 ℃ gradually decreased to a lower value in the steady-state regime. On the other hand, the friction coefficient measured for the Ni-P/SiC-500 coating slightly increased before to reach a steady-state value. These differences were attributed to the lower surface roughness exhibited by the coating annealed at 500 ℃ (Fig.3). In addition, the running-in period (P_r) for Ni-P/SiC-450 and Ni-P/SiC-500 coatings (around 300 s) was significantly shorter than that found for Ni-P/SiC-50 (900 s) and Ni-P/SiC-350 (1200 s) coatings. This is attributed to their smoother surface morphology, which reduced the time needed to remove large asperities. In order to characterize the friction behavior of Ni-P/SiC coatings, a mean-steady friction value (μ_m) was calculated as average over the steady-stage regime (see Fig.4b). The as-plated Ni-P/SiC-50 coating exhibited a μ_m of 0.54, while a slight increase (~0.55) occurred after annealing at 350 ℃. For higher annealing temperatures in the range of 350-500 ℃, μ_m gradually decreased from 0.55 to 0.51.

XRD patterns indicated that, for annealing temperatures above 350 ℃, the Ni_3P phase gradually formed in coatings. Compared with the oxidation reaction of Ni-P/SiC-50 and Ni-P/SiC-350 coatings (Eq. (2)), Ni-P/SiC-400, Ni-P-/SiC-450 and Ni-P/SiC-500 coatings experienced the oxidation reaction given as Eq. (3).

$$4Ni + 3O_2 = 2Ni_2O_3 \quad (2)$$

$$\Delta G_f^{298} = -287.6\ \text{kJ} \cdot \text{mol}^{-1}$$

$$2Ni_3P + 7O_2 = 3Ni_2O_3 + P_2O_5 \quad (3)$$

$$\Delta G_{\mathrm{f}}^{298} = -1364.7\ \mathrm{kJ \cdot mol^{-1}}$$

$$\mathrm{P_2O_5 + 3H_2O = 2H_3PO_4} \quad (4)$$

$$\Delta G_{\mathrm{f}}^{298} = -144.1\ \mathrm{kJ \cdot mol^{-1}}$$

As a generation of Eq. (3), P_2O_5 is extremely unstable and therefore can easily absorb water from the environment to form orthophosphoric acid (H_3PO_4) as determined in Eq. (4). Based on the literature, H_3PO_4 could have a significant effect on tribological behavior [36-38]. For instance, TiN/Al_2O_3 tribopair presented a low friction coefficient of 0.1 in H_3PO_4 compared to that measured in demineralised water (0.4), which was attributed to a lubricant gel containing Fe-P-O [36]. Likewise, Luo's group [37, 38] found a superlubricity phenomenon of Si_3N_4/glass tribopair with a friction coefficient of 0.004 measured in aqueous solution of H_3PO_4 (pH=1.5). It was concluded that the electrical double layer effect and the hydration effect on the positive charged surface caused the observed superlubrication. In our study, the formation of H_3PO_4 during sliding, especially in coatings annealed at the temperatures above 400 ℃, was responsible for the lower friction coefficient (see Fig. 4b). In particular, the Ni-P/SiC-500 coating with the highest Ni_3P content exhibited the lowest friction coefficient (0.51). The lower friction coefficient measured for Ni-P/SiC-450 and Ni-P/SiC-500 coatings was also attributed to the better surface quality achieved after polishing (Fig.3d-e). A similar result was reported in elsewhere [10].

3.4 Wear mechanisms

The wear rate (W_r) measured on Ni-P/SiC coatings (Fig.5a) exhibited a similar trend as that found for μ_m (Fig. 4b). In particular, Ni-P/SiC-350 coating exhibited the highest wear rate (6.1×10^{-5} mm^3/Nm) while Ni-P/SiC-500 coating presented the strongest wear resistance with the lowest wear rate of 7.8×10^{-6} mm^3/Nm. Generally, the wear resistance of coatings is proportional to the H as well as to H/E_r and H^3/E_r^2 ratios. However, Ni-P/SiC-500 with the lowest hardness, instead of Ni-P/SiC-400 with superior mechanical properties, exhibited the strongest wear resistance. As referred above, the H_3PO_4 produced from the tribochemical reaction not only reduced friction coefficient, but also contributed to the formation of Fe-P-O gel, thus preventing further wear. Therefore, a higher Ni_3P

content in Ni-P/SiC-500 coating resulted in a larger formation of H_3PO_4 with a subsequent reduction in both friction and wear. In addition, the Fe-P-O gel also contributed at protecting the counterparts, and therefore the wear rate of 52100 ball sliding against Ni-P/SiC-500 coating was only 2.9×10^{-7} mm^3/Nm. This wear rate was one order of magnitude lower (Fig.5b) compared to that found on balls used against coatings annealed at 350, 400 and 450 ℃ ($2.2\sim4.3\times10^{-6}$ mm^3/Nm).

On the other hand, during reciprocating sliding tests, wear debris were difficult to be removed from the wear track immediately and often they were pressed to form oxide films on the sliding surface. This is evident from the EDS measurements reported in Fig.6. All the wear tracks in this study were oxidized at different levels. Oxides were observed on the wear tracks of Ni-P/SiC-50 and Ni-P/SiC-350 coatings, while little oxides were found on the wear tracks of Ni-P/SiC-450 and Ni-P/SiC-500 coatings (Fig.7). As a result, the roughness (*R*a) of the wear tracks on Ni-P/SiC-50 and Ni-P/SiC-350 coatings (7.86~8.82 μm) were higher than that measured on the coatings annealed at 400, 450 and 500 ℃ (2.15~5.71 μm). Moreover, according to EDS analysis in Fig.6b', the wear debris on Ni-P/SiC-350 coating consisted of nickel and iron oxides, which instead were absent on the wear track of Ni-P/SiC-50 coating. Iron oxides were found to further deteriorate the contact surface, thus leading to the highest wear rate and *R*a (8.82 μm) for Ni-P/SiC-350 coating. For higher annealing temperatures (400-500 ℃), the wear track of individual coatings became smoother due to the tribochemical reaction mentioned above. In particular, the Ni-P/SiC-500 coating exhibited a wear track with the lowest oxygen content (9.1 at.%), thus suggesting less oxides adhered on the sliding surface. Consequently, the smoother interface (*R*a=2.15 μm) and the fewer oxides found on the wear track of the Ni-P/SiC-500 coating contributed to lower the wear rate.

4. Conclusions

Structural, mechanical and tribological properties of Ni-P/SiC nanocomposite coatings were investigated in relation to the post-deposition heat treatment and in particular as a function of the annealing temperature. Conclusions are drawn as follows:

(1) Regardless of the annealing temperature in the range of 350-500 ℃, a hard Ni_3P phase

formed in annealed coatings, thus causing an increase in hardness ranging from 7.1±0.6 to 8.2±0.5 GPa compared to the as-plated coating (6.3±0.3 GPa).

(2) Despite of the highest hardness (8.2 GPa), Ni-P/SiC coating annealed at 350 ℃ presented the worst tribological properties (μ=0.55 and W_r=6.1×10^{-5} mm^3/Nm) because of its rougher surface morphology and scarce formation of solid lubricant (H_3PO_4) from the tribochemical reaction owing to the lower Ni_3P content compared to the other coatings.

(3) The lubricating effect associated with the formation of H_3PO_4 in Ni-P/SiC coatings annealed at temperatures ≥ 400 °C, contributed to lower friction coefficient (0.51-0.54) and wear rate (4.3×10^{-5}-7.8×10^{-6} mm^3/Nm), while higher values were found for lower annealing temperatures.

(4) In spite of the lower hardness (7.1 GPa) compared to the other coatings, Ni-P/SiC-500 exhibited the lowest friction coefficient (0.51) and wear rate (7.8×10^{-6} mm^3/Nm) owing to a sufficient formation of solid lubrication (H_3PO_4) and to its better surface quality.

Acknowledgement

The research leading to these results has received funding from the European Union's Seventh Framework Research for SME Associations Programme under grant agreement No. 606110 (HardAlt).

Reference:

[1] K.G. Budinski, M.K. Budinski, Engineering Materials: Properties and Selection, Ninth ed., Prentice Hall, New York, 2010.

[2] B. Sonntag, V. Sundaram, Substitution of Cr (VI)-containing coatings by the European automobile industry. Indian Surf. Finish. 1 (2004) 15-26.

[3] M.D. Cohen, M. Costa, Chromium, in: M. Lippmann, Environmental Toxicants: Human Exposures and Their Health Effects, Second ed., Wiley, New York, 2000, pp. 173-191.

[4] B. Panja, P. Sahoo, Wear behavior of electroless Ni-P coatings in brine solution and optimization of coating parameters. Procedia Technol. 14 (2014) 173-180.

[5] R. Elansezhian, B. Ramamoorthy, P. K. Nair, Effect of surfactants on the mechanical properties of electroless (Ni-P) coating. Surf. Coat. Technol. 203 (2008) 709-712.

[6] W.L. Liu, S.H. Hsieh, T.K. Tsai, W.J. Chen, S.S. Wu, Temperature and pH dependence of the electroless Ni-P deposition on silicon. Thin Solid Films 510 (2006) 102-106.

[7] J.D. Lin, C.L. Kuo, C.J. Hsia, The influence of microwave-assisted hydrogen plasma treatment on electroless Ni-P coatings. Mater. Chem. Phys. 137 (2013) 848-858.

[8] M. Novak, D. Vojtech, P. Novak, T. Vitu, Tribological properties of heat-treated electroless Ni-P coatings on AZ91 alloy. Appl. Surf. Sci. 257 (2011) 9982-9985.
[9] S.S. Zhang, K.J. Han, L. Cheng, The effect of SiC particles added in electroless Ni-P plating solution on the properties of composite coatings. Surf. Coat. Technol. 202 (2008) 2807-2812.
[10] M. Franco, W. Sha, S. Malinov, H. Liu, Micro-scale wear characteristics of electroless Ni-P/SiC composite coating under two different sliding conditions. Wear 317 (2014) 254-264.
[11] I.R. Mafi, C. Dehghanian, Studying the effects of the addition of TiN nanoparticles to Ni-P electroless coatings. Appl. Surf. Sci. 258 (2011) 1876-1880.
[12] S.M.A. Shibli, V.S. Dilimon, Effect of phosphorous content and TiO_2-reinforcement on Ni-P electroless plates for hydrogen evolution reaction. Int. J. Hydrogen Energy 32 (2007) 1694-1700.
[13] S. Sadreddini, Z. Salehi, H. Rassaie, Characterization of Ni-P-SiO_2 nano-composite coating on magnesium. Appl. Surf. Sci. 324 (2015) 393-398.
[14] Z.A. Hamid, S.A.E. Badry, A.A. Aal, Electroless deposition and characterization of Ni-P-WC composite alloys. Surf. Coat. Technol. 201 (2007) 5948-5953.
[15] S. Alirezaei, S.M. Monirvaghefi, M. Salehi, A. Saatchi, Wear behavior of Ni-P and Ni-P-Al_2O_3 electroless coatings. Wear 262 (2007) 978-985.
[16] M.E. Hosseinabadi, K.A. Dorcheh, S.M.M. Vaghefi, Wear behavior of electroless Ni-P-B_4C composite coatings. Wear 260 (2006) 123-127.
[17] M. Alishahi, S.M. Monirvaghefi, A. Saatchi, S.M. Hosseini, The effect of carbon nanotubes on the corrosion and tribological behavior of electroless Ni-P-CNT composite coating. Appl. Surf. Sci. 258 (2012) 2439-2446.
[18] I.R. Aslanyan, J.P. Bonino, J.P. Celis, Effect of reinforcing submicron SiC particles on the wear of electrolytic Ni-P coatings Part 1: Uni-directional sliding. Surf. Coat. Technol. 200 (2006) 2909-2916.
[19] X.T. Yuan, D.B. Sun, H.Y. Yu, Y. Wang, Effect of nano-SiC particles on the corrosion resistance of Ni-P-SiC composite coatings. Int. J. Miner. Metall. Mater. 16 (2009) 444-451.
[20] A. Zoikis-Karathanasis, E.A. Pavlatou, N. Spyrellis, Pulse electrodeposition of Ni-P matrix composite coatings reinforced by SiC particles. J. Alloys Compd. 494 (2010) 396-403.
[21] H.L. Wang, L.Y. Liu, Y. Dou, W.Z. Zhang, W.F. Jiang, Preparation and corrosion resistance of electroless Ni-P/SiC functionally gradient coatings on AZ91D magnesium alloy. Appl. Surf. Sci. 286 (2013) 319-327.
[22] C.F. Malfatti, H.M. Veit, T.L. Menezes, J. Zoppas Ferreira, J.S. Rodrigu ês, J.P. Bonino, The surfactant addition effect in the elaboration of electrodeposited Ni-P-SiC composite coatings. Surf. Coat. Technol. 201 (2007) 6318-6324.
[23] Y.T. Wu, H.Z. Liu, B. Shen, L. Liu, W.B. Hu, The friction and wear of electroless Ni-P matrix with PTFE and/or SiC particles composite. Tribol. Int. 39 (2006) 553-559.
[24] C. F. Malfatti, H. M. Veit, C. B. Santos, M. Metzner, H. Hololeczek, J.P. Bonino, Heat treated Ni-P-SiC composite coatings: elaboration and tribocorrosion behaviour in NaCl solution. Tribol. Int. 36 (2009) 165-173.
[25] I. R. Aslanyan, J.P. Celis, L. Sh. Shuster, Effect of reinforcing submicron SiC particles on the wear process of electrolytic Ni-P coatings. J. Frict. Wear 31 (2010) 341-348.

[26] A. Amell, C. Muller, M. Sarret, Influence of fluorosurfactants on the codeposition of ceramic nanoparticles and the morphology of electroless Ni-P coatings. Surf. Coat. Technol. 205 (2010) 356-362.
[27] S.R. Allahkaram, M. H. Nazari, S. Mamaghani, A. Zarebidaki, Characterization and corrosion behavior of electroless Ni-P/nano-SiC coating inside the CO_2 containing media in the presence of acetic acid. Mater. Des. 32 (2011) 750-755.
[28] A. Farzaneh, M. Mohammadi, M. Ehteshamzadeh, F. Mohammadi, Electrochemical and structural properties of electroless Ni-P-SiC nanocomposite coatings, Appl. Surf. Sci. 276 (2013) 697-704.
[29] F. Bigdeli, S.R. Allahkaram, An investigation on corrosion resistance of as-applied and heat treated Ni-P/nano SiC coatings, Mater. Des. 30(10) (2009) 4450-4453.
[30] C.J. Lin, K.C. Chen, J.L. He, The cavitation erosion behavior of electroless Ni-P-SiC composite coating. Wear 261 (2006) 1390-1396.
[31] M. Sarret, C. Müller, A. Amell, Electroless Ni-P micro- and nano-composite coatings. Surf. Coat. Technol. 201 (2006) 389-395.
[32] R. Soleimani, F. Mahboubi, M. Kazemi, S.Y. Arman, Corrosion and tribological behaviour of electroless Ni-P/nano-SiC composite coating on aluminium 6061, Surf. Eng. 31(9) (2015) 714-721.
[33] D. Nava, C.E. Dávalos, A. Martínez-Hernández, F. Manríquez, Y. Meas, R. Ortega-Borges, J.J. Pérez-Bueno, G. Trejo, Effects of heat treatment on the tribological and corrosion properties of electrodeposited Ni-P alloys. Int. J. Electrochem. Sci. 8 (2013) 2670-2681.
[34] M.A. Meyers, A. Mishra, D.J. Benson, Mechanical properties of nanocrystalline materials. Prog. Mater. Sci. 51 (2006) 427-556.
[35] N.A. Sakharova, J.V. Fernandes, M.C. Oliveira, J.M. Antunes, Influence of ductile interlayers on mechanical behaviour of hard coatings under depth-sensing indentation: a numerical study on TiAlN. J. Mater. Sci. 45 (2010) 3812-3823.
[36] E. Wit, D. Drees, P.Q. Wu, J.P. Celis, Lubricating reaction products on TiN coatings during sliding wear in phosphoric acid. Surf. Coat. Technol. 135 (2000) 8-13.
[37] J.J. Li, C.H. Zhang, J.B. Luo, Superlubricity behavior with phosphoric acid-water network induced by rubbing. Langmuir 27 (2011) 9413-9417.
[38] J.J. Li, C.H. Zhang, L. Sun, X.C. Lu, J.B. Luo, Tribochemistry and superlubricity induced by hydrogen ions. Langmuir 28 (2012) 15816-15823.

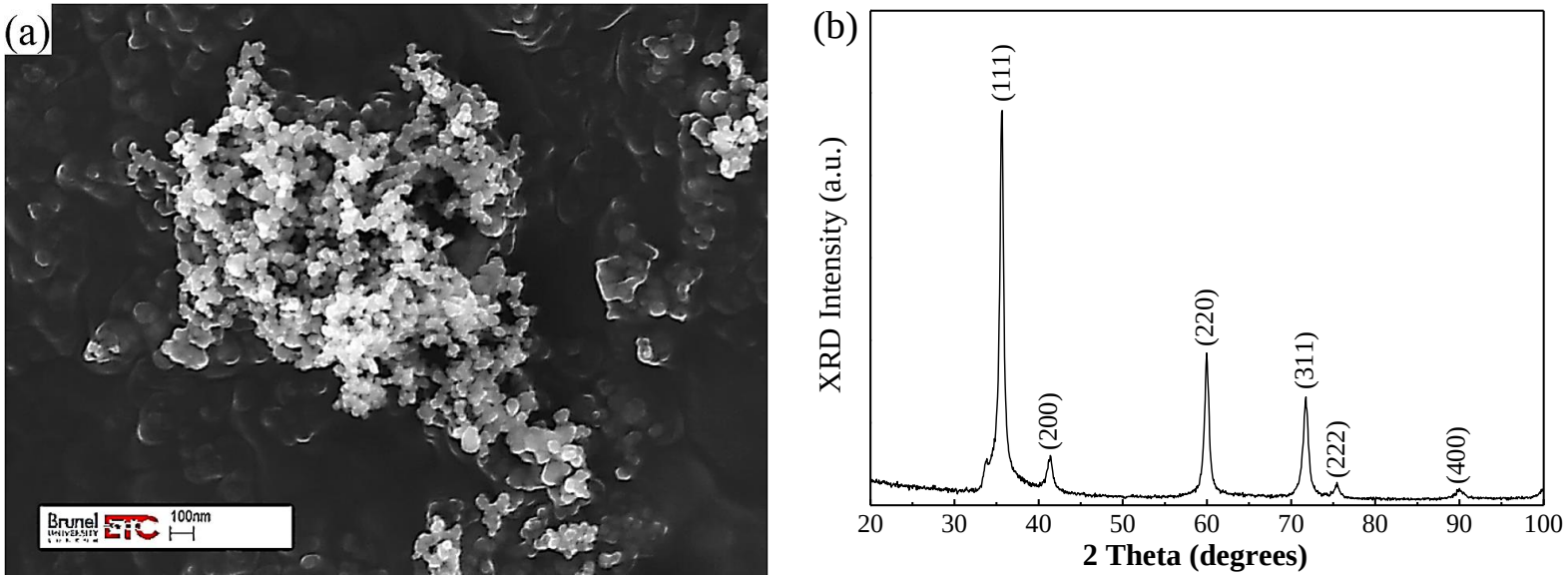

Fig.1 (a) FESEM image (b) XRD spectrum of β-SiC particles

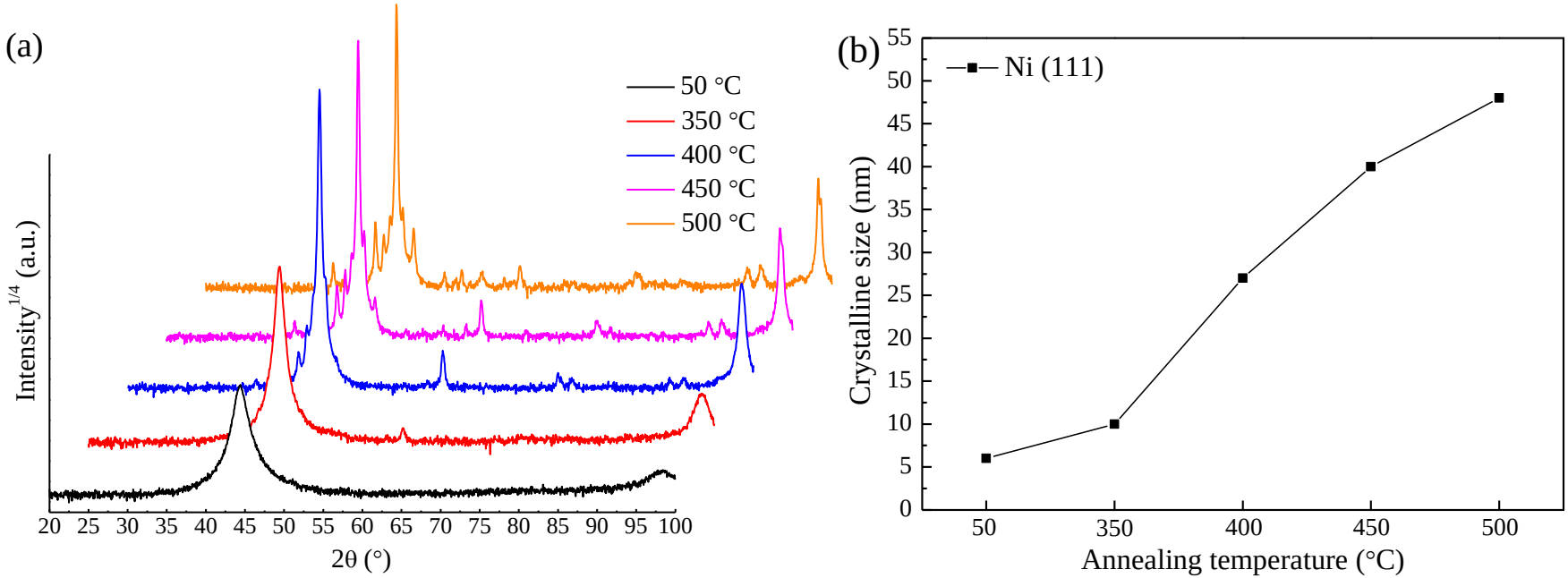

Fig.2 (a) XRD spectra of Ni-P/SiC coatings (b) Crystalline size of Ni (111) at different annealing temperatures

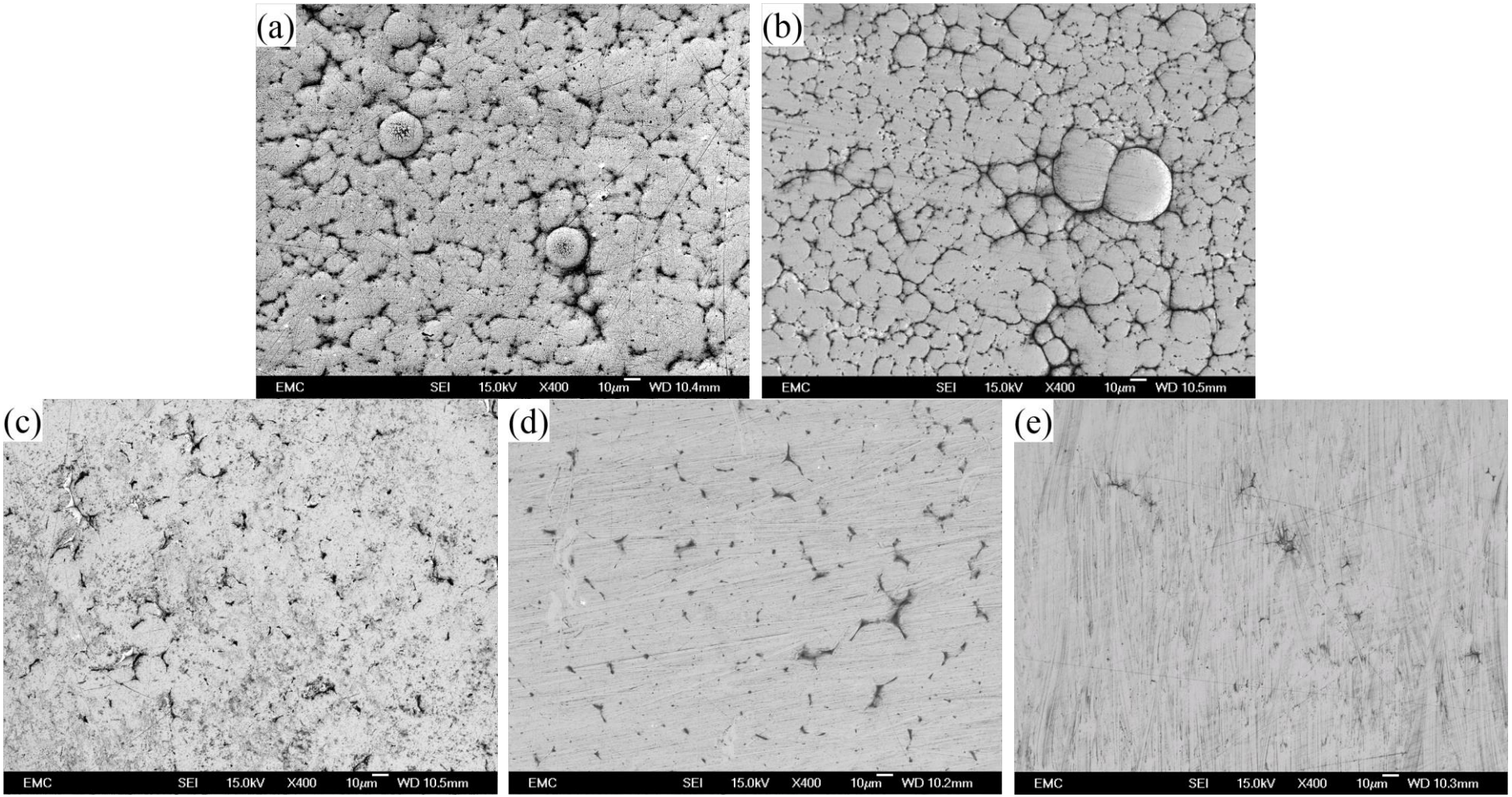

Fig.3 Morphology of the polished (a) Ni-P/SiC-50 (b) Ni-P/SiC-350 (c) Ni-P/SiC-400 (d) Ni-P/SiC-450 (e) Ni-P/SiC-500 coatings

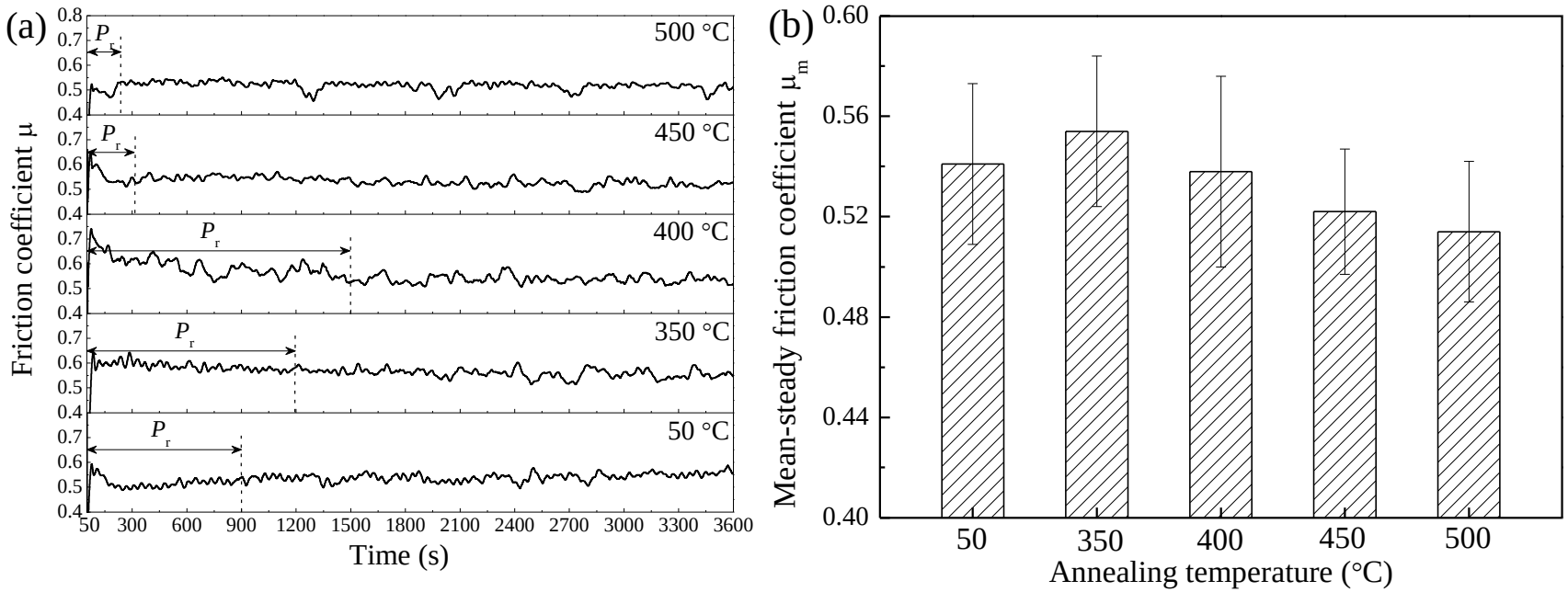

Fig.4 (a) Friction behavior (b) Mean-steady friction coefficient of Ni-P/SiC coatings at different annealing temperatures

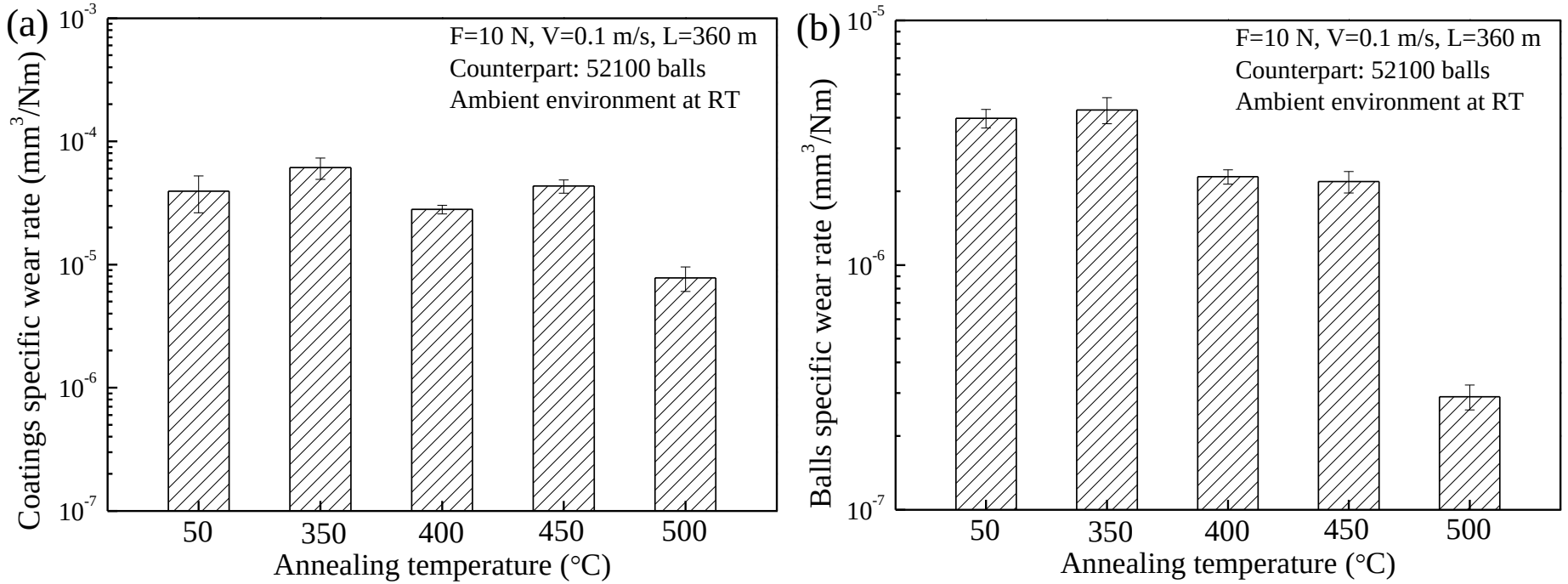

Fig.5 Specific wear rates of (a) Ni-P/SiC coatings and (b) 52100 balls at different annealing temperatures

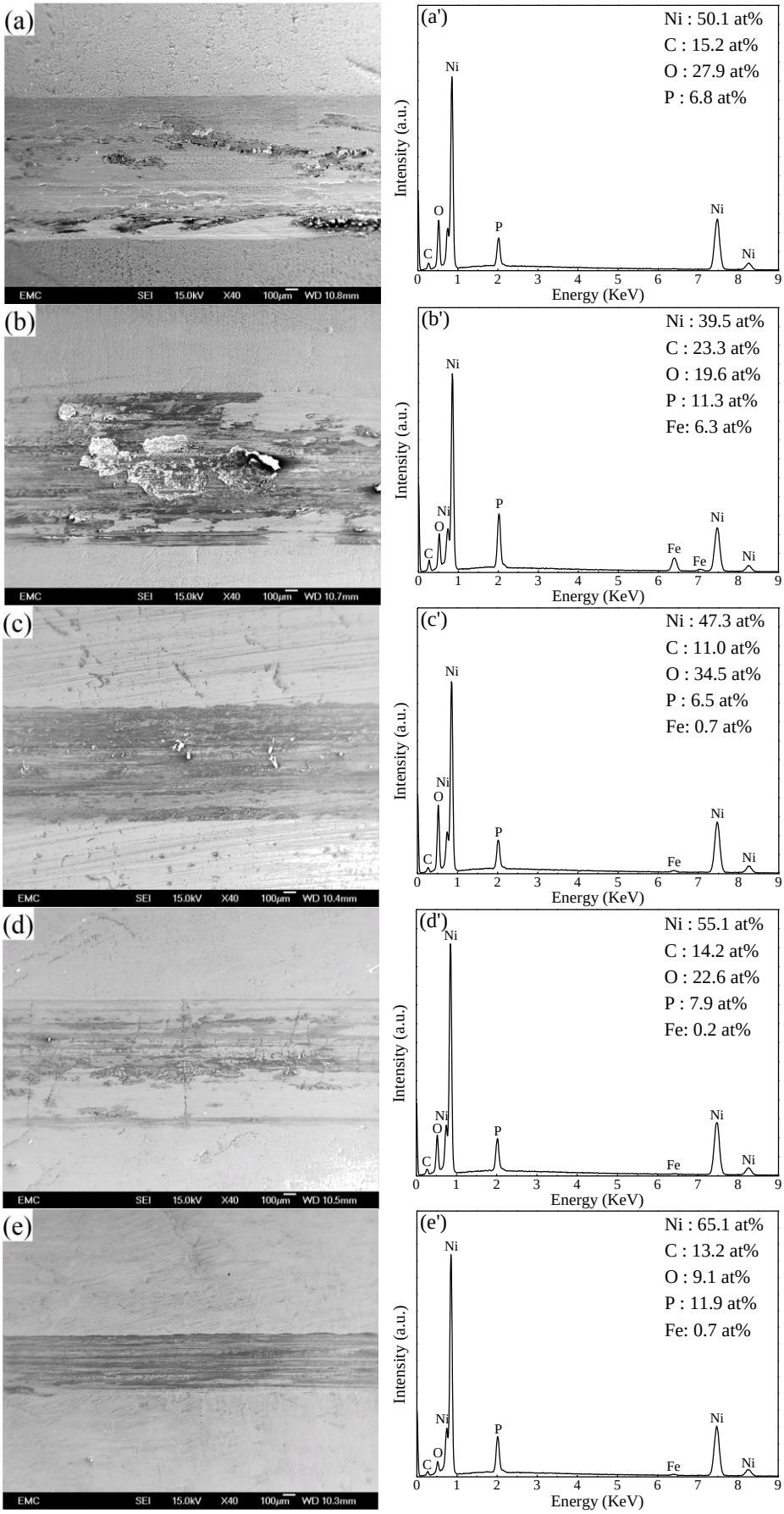

Fig.6 Overviews of wear tracks and EDS analyses on (a)(a') Ni-P/SiC-50 (b)(b') Ni-P/SiC-350 (c)(c') Ni-P/SiC-400 (d)(d') Ni-P/SiC-450 (e)(e') Ni-P/SiC-500 coatings

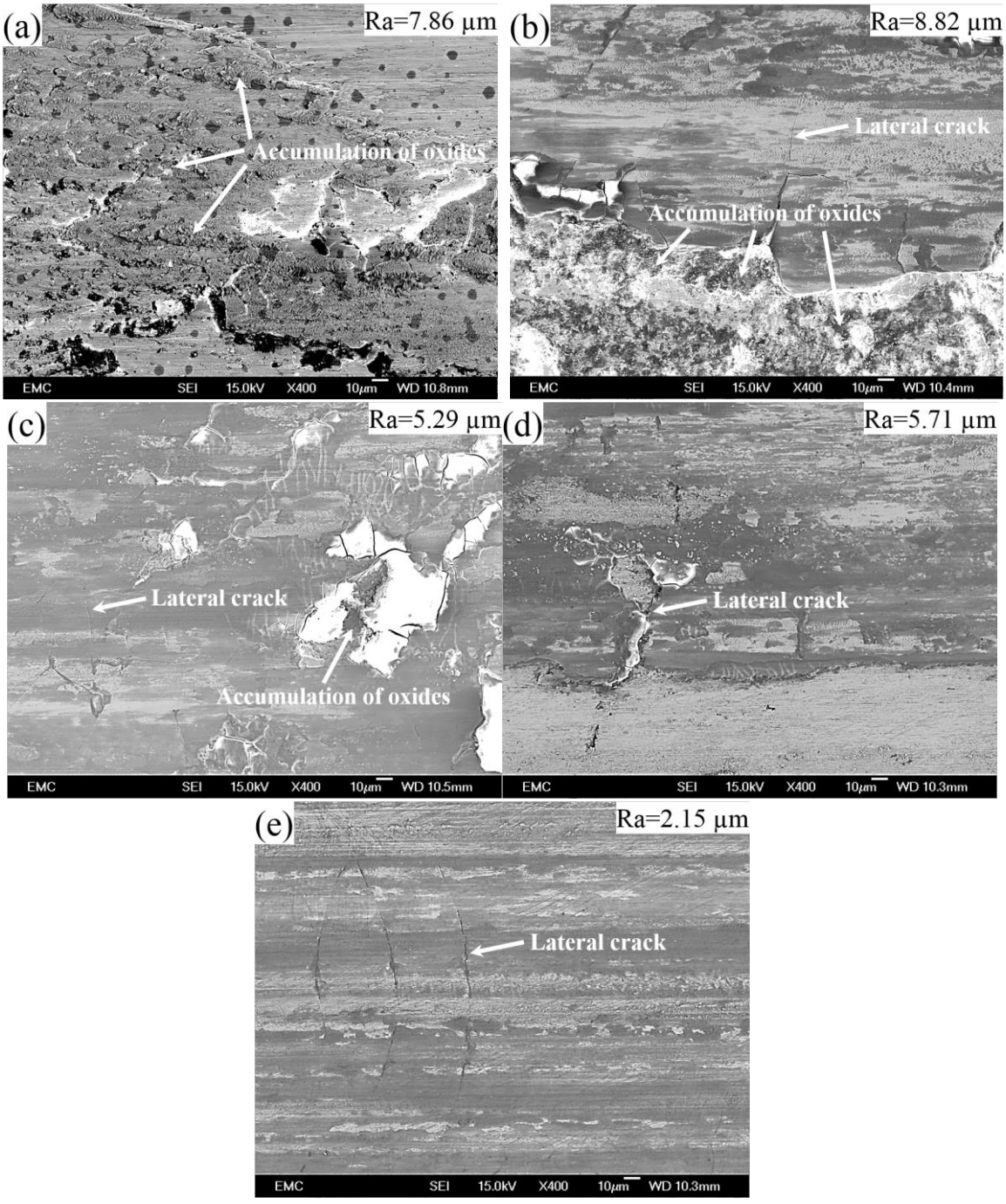

Fig.7 SEM images of partial wear tracks on (a) Ni-P/SiC-50 (b) Ni-P/SiC-350 (c) Ni-P/SiC-400 (d) Ni-P/SiC-450 (e) Ni-P/SiC-500 coatings

Table 1 Mechanical properties of Ni-P composite coatings reinforced by different particles

Reference	Particles	Loading (g/L)	Hardness of Ni-P (Hv)	Hardness of Ni-P composite (Hv)	Δ of hardness (Hv)
Zhang et al. [9]	SiC	12.0	530	809	279
Mafi et al. [11]	TiN	1.0	561	660	99
Shibli et al. [12]	TiO_2	12.0	429	553	124
Sadreddini et al. [13]	SiO_2	12.5	342	429	87
Hamid et al. [14]	WC	12.5	465	650	185
Alirezaei et al. [15]	Al_2O_3	15.0	475	700	225
Hosseinabadi et al. [16]	B_4C	4.0	640	720	80
Alishahi et al. [17]	CNT	2.0	538	800	262

Table 2 Electro-deposition conditions of Ni-P/SiC coatings

Temperature	50 ±2 ^{o}C
pH	1 ±0.2
SiC load	5 g/L
Current density	20 Adm^{-2}
Substrate	Steel platelet
Anode	Nickel (S)

Table 3 Phase conditions of the as-plated Ni-P/SiC coating and Ni-P/SiC coating annealed at 450 ℃

Coatings	**Ni-P/SiC-50**																
2 Theta (°)	--	--	--	--	44.43	--	--	--	--	--	--	--	--	--	--	--	98.33
Intensity (%)	--	--	--	--	100	--	--	--	--	--	--	--	--	--	--	--	4.5
Phase	--	--	--	--	Ni	--	--	--	--	--	--	--	--	--	--	--	Ni
hkl	--	--	--	--	111	--	--	--	--	--	--	--	--	--	--	--	222
Coatings	**Ni-P/SiC-450**																
2 Theta (°)	36.38	41.80	42.80	43.68	44.46	45.22	46.66	50.54	55.39	58.27	60.16	66.00	74.97	76.74	89.24	90.89	98.42
Intensity (%)	0.1	0.7	1.3	2.2	100	4.1	0.4	0.1	0.1	0.1	0.4	0.1	0.1	0.1	0.1	0.1	4.4
Phase	Ni_3P	Ni_3P	Ni_3P	Ni_3P	Ni	Ni_3P	Ni_3P	Ni_3P	Ni_3P	Ni_3P	Ni_3P	Ni_3P	Ni_3P	Ni_3P	Ni_3P	Ni_3P	Ni
hkl	031	231	330	112	111	240	141	222	341	440	332	620	233	460	172	462	222

Table 4 Mechanical properties of Ni-P/SiC coatings at different annealing temperatures

Coatings	H **(GPa)**	E_r **(GPa)**	H/E_r	H^3/E_r^2 **(GPa)**
Ni-P/SiC-50	6.3±0.3	158±8	0.040	0.010
Ni-P/SiC-350	8.2±0.5	192±7	0.043	0.015
Ni-P/SiC-400	8.2±0.3	156±5	0.053	0.023
Ni-P/SiC-450	7.8±0.3	191±8	0.041	0.013
Ni-P/SiC-500	7.1±0.6	214±9	0.033	0.008